Geologic Map of the Mammoth 7½' Quadrangle, Pinal County, Arizona

by

Jon E. Spencer, Brian F. Gootee, Stephen M. Richard,
and Joseph P. Cook

Arizona Geological Survey Digital Geologic Map DGM-67

version 1.0

September, 2009

Scale 1:24,000 (1 sheet, with text)

Arizona Geological Survey
416 W. Congress St., #100, Tucson, Arizona 85701

This geologic map was funded in part by the USGS National Cooperative Geologic Mapping Program, award no. 07HQAG0110. The views and conclusions contained in this document are those of the authors and should not be interpreted as necessarily representing the official policies, either expressed or implied, of the U.S. Government.

Geologic Map of the Mammoth 7½' Quadrangle, Pinal County, Arizona

by

Jon E. Spencer, Brian F. Gootee, Stephen M. Richard,
and Joseph P. Cook

INTRODUCTION

The Mammoth 7½' Quadrangle includes part of the San Pedro River, flanking valley fill, and bedrock on the west side of the valley that forms the Black Hills and the northernmost tip of the Santa Catalina Mountains (Figure 1). Production of this new geologic map continues the Arizona Geological Survey mapping program of the San Pedro River valley. This mapping was done under the joint State-Federal STATEMAP program, as specified in the National Geologic Mapping Act of 1992, and was jointly funded by the Arizona Geological Survey and the U.S. Geological Survey under STATEMAP Program Contract award number 07HQAG0110. Mapping was compiled digitally using ESRI ArcGIS software.

The Mammoth Quadrangle was mapped previously by Creasey (1965, 1967) and Dickinson (1993). Other mapping of specific areas in the Quadrangle include that by Peterson (1938), Heindl (1963), Weibel (1982), and Force (1997). Structural studies of the dismembered San Manuel – Kalamazoo ore body included those by Lowell (1968), Force and Cox (1992), Force et al. (1995), Guilbert and Lowell (1995), and Dickinson et al. (1995). Regional tectonic and structural setting is described by Dickinson and Shafiqullah (1987), Dickinson (1991), and Davis et al. (2004). New mapping presented in this study was focused on the late Cenozoic geology of the region, especially Quaternary units along the San Pedro River and on the lower valley flanks. New mapping was also done in the Tiger Mine area to determine the nature of breccias and their relationship to faulting and mineralization. Cross sections presented here are intended to show the geometry of Tertiary normal faults, and extend to the west onto the adjacent North of Oracle 7.5' Quadrangle (Orr et al., 2004).

Bedrock geology

Bedrock in the Mammoth 7.5' Quadrangle consists largely of Mesoproterozoic Oracle Granite and related aplite dikes, alaskite, and granodiorite. The granodiorite is suspected to be a phase of the Oracle Granite as they are somewhat similar in appearance, both are cut by aplite dikes and an alaskite intrusion thought to be related to the Oracle Granite, and both are undeformed by foliation that commonly affects Paleoproterozoic rocks in the region. Bedrock was cut and tilted by several Oligo-Miocene normal faults, with deposition of the volcanic and conglomeratic Cloudburst Formation during the first episode of faulting and deposition of San Manual Formation sandstone and conglomerate during the second (e.g., Dickinson, 1991). The upper Miocene to Pliocene Quiburis Formation was deposited in the San Pedro River valley while the valley was hydrologically closed and a lake was present in the valley (Dickinson, 2003). Integration with the Gila River was followed by incision that has shaped the modern landscape.

New bedrock mapping was directed at determining the significance of breccias in the Tiger Mine area. This new work led us to the conclusion that breccias were produced by magmatic processes probably associated with gas-charged magmas or gas eruption during magma eruption. A rhyolite unit is strongly associated with the brecciation. In the Tiger mine area, rhyolite, mafic lavas, and Oracle Granite are all brecciated, with varying amounts of each unit in the breccias. Whereas rhyolite and Oracle Granite were apparently carried upward during brecciation, breccias derived from Cloudburst volcanics can not have been carried upward more than a few tens to perhaps a hundred meters because the underlying Cloudburst detachment fault forms the lower bound of the Cloudburst volcanics. Thus we consider it possible that some of the mafic-volcanic breccias represent debris that fell into vents left open by gas-rich eruptions. The rhyolite was analyzed for major and trace elements because of its association with mineralization in the Tiger mine area (Figure 2; Tables 1, 2, and 3).

The breccias and rhyolites in the Tiger mine area were emplaced across the east-northeast striking Turtle fault, and so post-date the fault. The Turtle fault was thought to form a lateral ramp to the Cloudburst fault, with the subhorizontal Cloudburst fault changing from subhorizontal to the north to steeply north-dipping to the south (Dickinson, 1991; Force, 1997). However, alteration in the immediate footwall of the Cloudburst fault is moderately to strongly chloritic, whereas alteration in the footwall of the Turtle fault is weak and hematitic. This change in footwall alteration, combined with the abrupt change in fault orientation, lead us to conclude that the Turtle fault is a younger, north-side-down normal fault that cuts and displaces the Cloudburst fault. In this interpretation the southward continuation of the Cloudburst fault in the footwall of the Turtle fault must have been eroded away.

The hanging wall of the Cloudburst detachment fault consists of volcanic and sedimentary rocks of the Cloudburst Formation, which were mapped separately by Creasey (1965). However, the complex structural and stratigraphic relationships between these two units are not shown on the map accompanying this report.

Cross sections presented here show the feasibility of southeastward-increasing displacement on the San Manuel fault. The Cloudburst detachment fault was recognized in the hanging wall of the San Manuel fault west of Signal Peak (located in the northwestern corner of the Mammoth 7.5' Quadrangle) in the adjacent North of Oracle 7.5' Quadrangle (Orr et al., 2004). Westward projection of the Cloudburst detachment fault over Signal Peak (cross-section B), to the point where it would be cut off by the upward projection of the San Manuel fault, places this cutoff at probably less than one kilometer up-dip (on the San Manuel fault) from the Cloudburst detachment fault farther west. This contrasts with the ~2.4 km separation of the San Manuel and Kalamazoo ore bodies, which is thought to have originated as a single ore body (Lowell, 1968; Lowell and Guilbert, 1970). These two offset estimates are reconciled if displacement on the San Manuel fault increases southeastward, with ~15° of clockwise rotation of the hanging wall relative to the footwall. With this geometry, the pivot point where San Manuel fault displacement dies out to zero is located 1.7 km northwest of the point where the San Manuel fault crosses cross-section A and at about the point where it intersects the Cowhead Well fault (Orr et al., 2004).

Upper Cenozoic deposits

The northeastern portion of the Mammoth Quadrangle is underlain by late Cenozoic, valley-filling clastic and chemical sedimentary strata of the Quiburis Formation (Dickinson, 1998, 2003). These consist mostly of sand and conglomeratic debris in alluvial fans that flank the San Pedro valley and an axial valley facies including both fine-grained sandflat and fan toe and lacustrine sedimentary units. Less common, well preserved ash deposits and diatomite beds are found throughout stratigraphic intervals in the lacustrine facies within the Mammoth Quadrangle. Each facies of the Quiburis Formation is interpreted to have an interfingering relationship, where interbedded lithologies commonly mark the lateral transition from one facies to another. The uppermost exposures of the lacustrine and sandflat facies are overlain basin-ward by the sandflat and conglomeratic facies respectively, thus interpreted to represent a progradational event of clastic sediment onlap near the end of a basin-filling episode.

Integration of the San Pedro drainage system with the Gila River terminated basin-filling sedimentation and began a period of incision that continues to the present (Dickinson, 2003). Geomorphic modification of the valley during incision has produced a complex Quaternary landscape with many Quaternary units reflecting different periods of Quaternary aggradation and incision.

Geologic hazards

Geologic hazards within the map area include flooding in the San Pedro River channel, flash flooding from tributaries to the San Pedro River and potential groundwater contamination from mine tailings. Flooding in the San Pedro River corridor is restricted to a valley floor that is delineated on both sides by a bluff approximately 10 to 15 meters above Holocene river and tributary alluvial fan deposits. Tributaries are capable of transporting coarse sand and gravel and occasionally cobbles in response to runoff from flash floods following intense thunderstorms. Contamination from mine tailings presents a potential long-term hazard to groundwater and to the lower San Pedro River.

Other geologic hazards include soil expansion, soil creep, and small landslides and dust. Soil expansion can occur where there is substantial soil clay accumulation, which is common in map units Qi2 and Qi3 (terrace deposits). Soil creep can occur on gentle to steep slopes associated with silt, mud or clay, which is widespread in the Quiburis sandflat and lacustrine facies. The sandflat and lacustrine facies of the Quiburis Formation contain substantial amounts of gypsum, which is quite soluble. Wetting of these deposits may result in gypsum dissolution and soil compaction or collapse. Small landslides can occur in areas where cliffs of loose material are undercut by erosion. An uncommon geologic hazard unique to the mapping area may include silicosis due to prolonged exposure to silica-rich dust generated from diatomite and volcanic ash beds common in the lacustrine facies of Quiburis formation, which is more abundant east of the San Pedro River and in the Clark Ranch Quadrangle. For more information on the character and mitigation of many of the aforementioned geologic hazards, see AZGS Down-to-Earth series No. 13 (Harris and Pearthree, 2002).

REFERENCES

Creasey, S. C., 1965, Geology of the San Manuel area, Pinal County, Arizona: U. S. Geological Survey Professional Paper 471, 64 p., with map, scale 1:24,000.

Creasey, S.C., 1967, General geology of the Mammoth Quadrangle, Pinal County, Arizona: U.S. Geological Survey Bulletin 1218, 94 p., plate 1 scale 1:48,000.

Davis, G.H., Constenius, K.N., Dickinson, W.R., Rodíguez, E.P., and Cox, L.J., 2004, Fault and fault-rock characteristics associated with Cenozoic extension and core-complex evolution in the Catalina-Rincon region, southeastern Arizona: Geological Society of America Bulletin, v. 116, n. 1/2, p. 128-141.

Dickinson, W.R., 1991, Tectonic setting of faulted Tertiary strata associated with the Catalina core complex in southern Arizona: Geological Society of America, Special Paper 264, 106 p.

Dickinson, W.R., 1993, Summary geologic map of Black Hills near Mammoth, Pinal County, Arizona [Mammoth 7.5 min]: Arizona Geological Survey Contributed Map CM-93-B, 1 sheet, scale 1:24,000.

Dickinson, W.R., 1998, Facies map of post-mid-Miocene Quiburis Formation, San Pedro trough, Pinal, Pima, Gila, Graham, and Cochise Counties, Arizona: Arizona Geological Survey Contributed Map CM-98-A, Ten sheets, scale 1:24,000, with 6 p. text.

Dickinson, W.R., 2003, Depositional facies of the Quiburis Formation, basin fill of the San Pedro trough, southeastern Arizona Basin and Range Province, *in* Raynolds, R.G., and Flores, R.M., eds., 2003, Cenozoic systems of the Rocky Mountain region: Denver, Rocky Mountain Section, SEPM (Society for Sedimentary Geology), p. 157-181.

Dickinson, W.R., and Shafiqullah, M., 1989, K-Ar and F-T ages for syntectonic mid-Tertiary volcanosedimentary sequences associated with the Catalina core complex and San Pedro trough in southern Arizona: Isochron/West, n. 52, p. 15-27.

Dickinson, W.R., Force, E.R., and Hagstrum, J.T., 1995, Tilting history of the San Manuel-Kalamazoo porphyry system, southeastern Arizona - A reply: Economic Geology, v. 90, no. 7, p. 2096-2098.

Force, E.R., 1997, Geology and mineral resources of the Santa Catalina Mountains, southeastern Arizona: Tucson, Arizona, Center for Mineral Resources, Monographs in Mineral Resource Science, n. 1, 134 p.

Force, E.R., and Cox, L.J., 1992, Structural context of mid-Tertiary mineralization in the Mammoth and San Manuel districts, southeastern Arizona: U.S. Geological Survey Bulletin 2042C, 28 p.

Force, E.R., Dickinson, W.R., and Hagstrum, J.T., 1995, Tilting history of the San Manuel-Kalamazoo porphyry system, southeastern Arizona: Economic Geology, v. 90, n. 1, p. 67-80.

Guilbert, J.M., and Lowell, J.D., 1995, Tilting history of the San Manuel-Kalamazoo porphyry system, southeastern Arizona - A discussion: Economic Geology, v. 90, no. 7, p. 2094-2096.

Harris, R.C., and Pearthree, P.A., 2002, A home buyer's guide to geologic hazards in Arizona: Arizona Geological Survey, Down-to-Earth Series, v. 13 (DTE-13), 36 p.

Heindl, L.A., 1963, Cenozoic geology in the Mammoth area, Pinal County, Arizona: U.S. Geological Survey Bulletin 1141-E, p. E1-E41, 3 sheets, scale 1:63,360.

Le Bas, M.J., Le Maitre, R.W., Streckeisen, A., and Zanettin, B., 1986, A chemical classification of volcanic rocks based on the total alkali-silica diagram: Journal of Petrology, v. 27, p. 745-750.

Lowell, J.D., 1968, Geology of the Kalamazoo orebody, San Manuel district, Arizona: Economic Geology, v. 63, no. 6, p. 645-654.

Lowell, J.D., and Guilbert, J.M., 1970, Lateral and vertical alteration-mineralization zoning in porphyry ore deposits: Economic Geology, v. 65, no. 4, p. 373-408.

Orr, T.R., Shipman, T.C., and Spencer, J.E., 2004, Geologic map of the North of Oracle 7 ½' Quadrangle, southeastern Pinal County, Arizona: Arizona Geological Survey Digital Geologic Map 23, v. 2.0, scale 1:24,000.

Peterson, N.P., 1938, Geology and ore deposits of the Mammoth mining camp area, Pinal County, Arizona: Arizona Bureau of Mines Bulletin, n. 144, 63 p., 10 sheets, scales 1:1,800 and 1:4,500.

Richard, S.M., and Kneale, S.M., 2003, Geologic map of Arizona: Arizona Geological Survey Digital Information Series DI-8, version 3 (includes ESRI ArcInfo export files, Microsoft Access 2000 database, ESRI ArcView 3.2 Project).

Unruh, D.M., 1997, Porphyry geochronology and geochemistry, *in* Force, E.R., Geology and mineral resources of the Santa Catalina Mountains, southeastern Arizona: Tucson, Arizona, Center for Mineral Resources, Monographs in Mineral Resource Science, n. 1, p. 94-100.

Weibel, W.L., 1981, Depositional history and geology of the Cloudburst Formation near Mammoth, Arizona: Tucson, University of Arizona, M.S. thesis, 81 p.

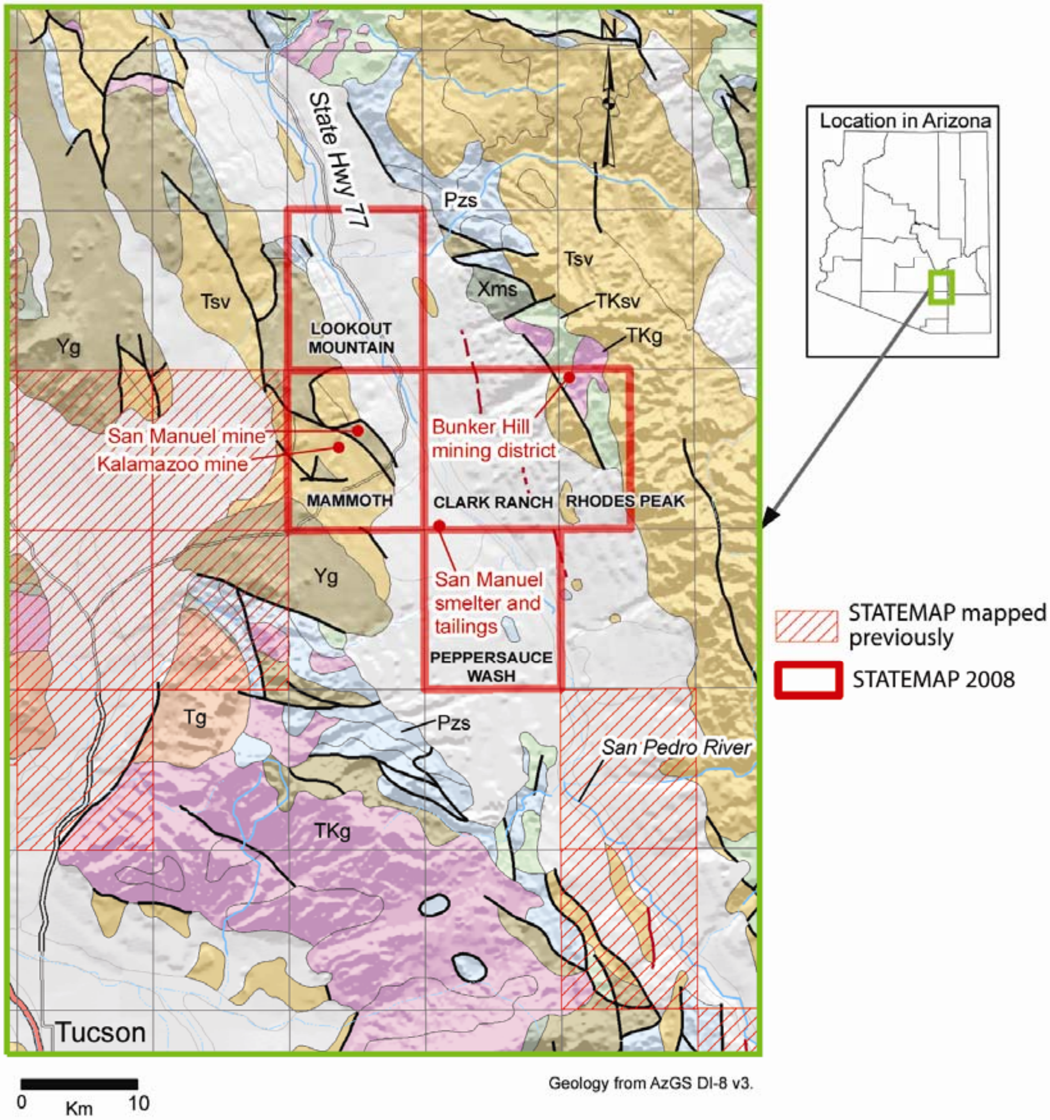

Tsv - Oligo-Miocene sedimentary and volcanic rocks
Tg - Oligo-Miocene granitic rocks
TKg - Early Tertiary and late Cretaceous (Laramide) granitic rocks
TKsv - Early Tertiary and Cretaceous sedimentary and volcanic rocks
Pzs - Paleozoic sedimentary rocks
Yg - Mesoproterozoic granitic rocks
Xms - Paleoprotoerozoic metasedimentary rocks

Figure 1. Geologic map of the lower San Pedro River valley area, southeastern Arizona, showing STATEMAP 2008 map areas.

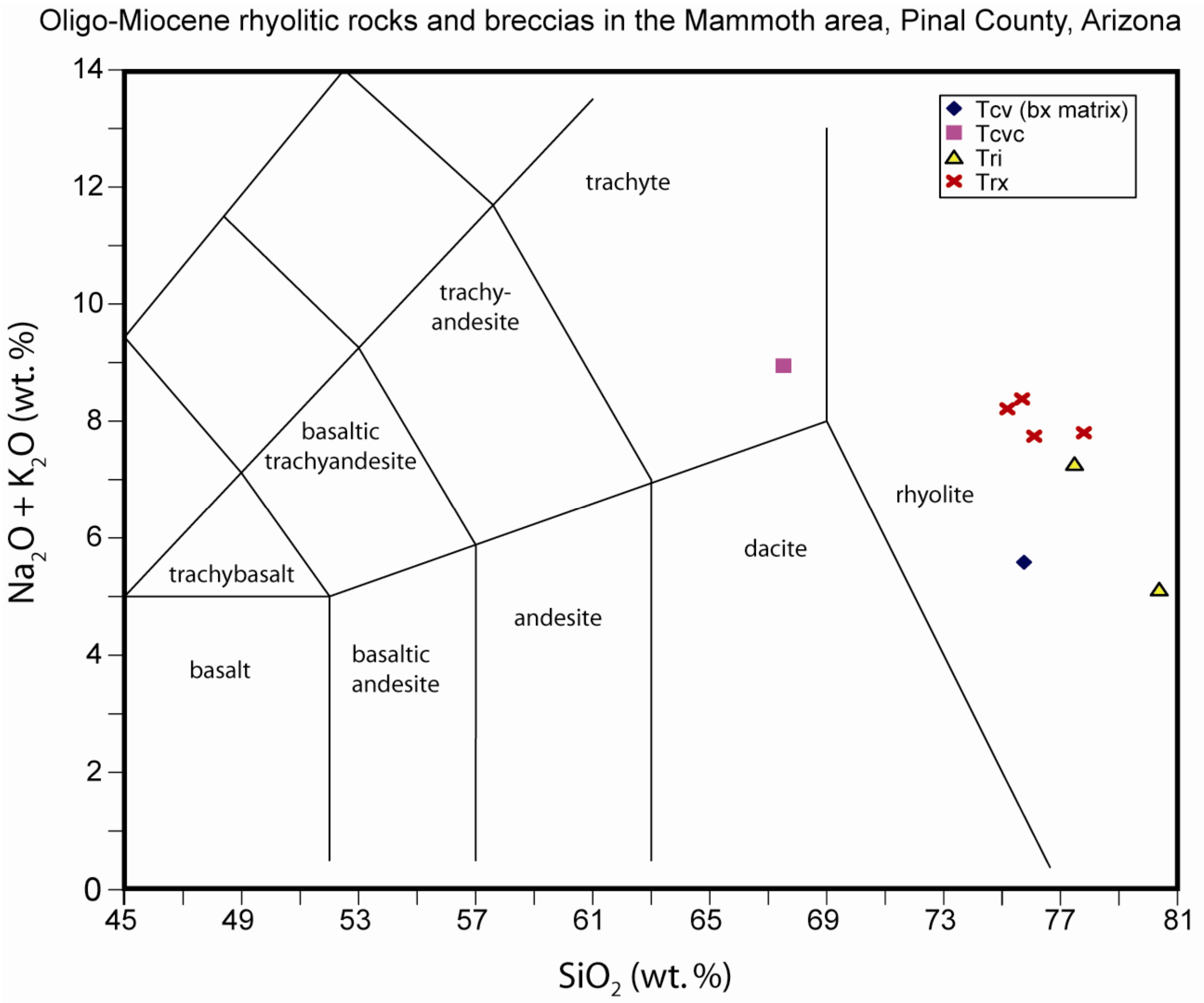

Figure 2. Geochemical classification diagram (from Le Bas et al., 1986) for selected volcanic and shallow intrusive rocks in the Mammoth 7 ½′ Quadrangle. See Plate 1 or text for corresponding unit names and locations.

TABLE 1. MAJOR-ELEMENT CHEMISTRY

Sample number	map unit	SiO_2 (%)	Al_2O_3 (%)	Fe_2O_3(T) (%)	MnO (%)	MgO (%)	CaO (%)	Na_2O (%)	K_2O (%)	TiO_2 (%)	P_2O_5 (%)	LOI (%)	Total (%)	Ba (ppm)	Sr (ppm)	Y (ppm)	Sc (ppm)	Zr (ppm)	Be (ppm)	V (ppm)
3-26-08-3	Tcv (bx matrix)	75.8	12.09	0.82		0.25	0.48	0.27	5.31		0.03	3.31	98.49		35			86		< 5
3-26-08-6	Tcvc	67.56	16.33	3.63	0.031	1.07	1.44	7.79	1.17	0.585	0.24	1.19	101	372	696	31	7	430	3	53
3-26-08-2	Tri	80.43	10.24	1.03		0.18	0.19	2.84	2.28		0.03	1.12	98.42		165			75		< 5
3-26-08-5	Tri	77.53	11.87	0.87		0.21	0.28	3.47	3.81		0.02	1.06	99.22		142			99		< 5
3-27-08-1	Trx	75.73	12.52	1.01		0.06	0.27	3.31	5.08		0.05	0.59	98.78		10			84		< 5
3-27-08-2	Trx	75.23	12.48	0.95		0.2	0.33	3.49	4.73		0.02	1.15	98.78		6			87		6
3-27-08-3	Trx	76.15	12.08	0.8		0.14	0.38	2.54	5.21		0.01	1.45	98.87		12			83		< 5
3-27-08-4	Trx	77.85	11.39	1		0.05	0.31	3.45	4.36		0.03	0.27	98.87		11			81		< 5
Detection Limit		0.01	0.01	0.01	0.001	0.01	0.01	0.01	0.01	0.001	0.01		0.01	2	2	1	1	2	1	5

All analyses by Activation Laboratories Ltd.

Sample preparation by lithium metaborate/tetraborate fusion. Analysis by inductively coupled plasma - mass spectrometry (Actlab whole-rock package code 4B (2008))

TABLE 2. TRACE-ELEMENT ANALYSES

Analyte Symbol		MnO	TiO2	Au	Ag	As	Ba	Be	Bi	Br	Cd	Co	Cr	Cs	Cu	Hf	Hg	Ir	Mo	Ni	Pb
Unit Symbol		%	%	ppb	ppm	ppm	ppm	ppm	ppm	ppm	ppm	ppm	ppm	ppm	ppm	ppm	ppm	ppb	ppm	ppm	ppm
Detection Limit		0.01	0.005	5	0.5	2	3	1	2	1	0.5	1	1	0.5	1	0.5	1	5	2	1	5
Analysis Method*		FUS-ICP	FUS-ICP	INAA	MULT INAA / TD-ICP	INAA	MULT INAA / FUS-ICP	FUS-ICP	TD-ICP	INAA	TD-ICP	INAA	INAA	INAA	TD-ICP	INAA	INAA	INAA	TD-ICP	TD-ICP	TD-ICP
sample number	map unit																				
3-26-08-3	Tcv (bx matrix)	0.04	0.095	6	< 0.5	3	415	4	< 2	< 1	< 0.5	3	85	23	43	5	< 1	< 5	< 2	7	9
3-26-08-2	Tri	0.02	0.075	< 5	< 0.5	3	117	7	< 2	< 1	< 0.5	3	26	4	18	4	< 1	< 5	< 2	2	< 5
3-26-08-5	Tri	0.03	0.055	< 5	< 0.5	5	154	3	< 2	< 1	< 0.5	3	26	5	6	4	< 1	< 5	< 2	4	< 5
3-27-08-1	Trx	0.07	0.088	< 5	< 0.5	10	61	7	< 2	< 1	< 0.5	3	100	9	6	4	< 1	< 5	< 2	5	22
3-27-08-2	Trx	0.1	0.081	< 5	< 0.5	6	25	9	< 2	< 1	< 0.5	3	17	10	3	5	< 1	< 5	< 2	2	27
3-27-08-3	Trx	0.04	0.077	< 5	< 0.5	15	21	7	< 2	< 1	< 0.5	< 1	40	12	2	5	< 1	< 5	< 2	2	19
3-27-08-4	Trx	0.09	0.077	< 5	< 0.5	17	35	7	< 2	< 1	< 0.5	< 1	23	10	2	4	< 1	< 5	< 2	3	28

TABLE 2. TRACE-ELEMENT ANALYSES, CONTINUED

Analyte Symbol		Rb	S	Sb	Sc	Se	Ta	Th	U	W	Y	Zn	La	Ce	Nd	Sm	Eu	Tb	Yb	Lu	Mass
Unit Symbol		ppm	%	ppm	ppm	ppm	ppm	ppm	ppm	ppm	ppm	ppm	ppm	ppm	ppm	ppm	ppm	ppm	ppm	ppm	g
Detection Limit		20	0.001	0.2	0.1	3	1	0.5	0.5	3	1	1	0.2	3	5	0.1	0.1	0.5	0.1	0.05	
Analysis Method*		INAA	TD-ICP	INAA	INAA	INAA	INAA	INAA	INAA	INAA	FUS-ICP	TD-ICP	INAA	INAA	INAA	INAA	INAA	INAA	INAA	INAA	INAA
sample number	map unit																				
3-26-08-3	Tcv (bx matrix)	390	0.024	1.5	3.6	< 3	4	51.9	8.3	< 3	27	35	34.3	39	11	3.2	0.6	< 0.5	5.2	0.77	1.38
3-26-08-2	Tri	180	0.003	0.7	2.6	< 3	< 1	41.8	4.9	< 3	33	34	26.5	43	10	3.2	< 0.1	< 0.5	4.8	0.75	1.37
3-26-08-5	Tri	210	0.006	0.6	4.2	< 3	< 1	38	3.8	< 3	31	37	18.9	40	17	6.6	0.3	1	4.8	0.68	1.31
3-27-08-1	Trx	370	0.007	0.4	3	< 3	3	43.6	4.5	< 3	39	35	23.4	44	7	2.9	< 0.1	< 0.5	5.2	0.77	1.47
3-27-08-2	Trx	400	0.002	0.4	3.7	< 3	5	41.7	7.2	4	38	37	20.4	47	< 5	2.1	< 0.1	< 0.5	5.5	0.8	1.58
3-27-08-3	Trx	470	0.003	1.2	4	< 3	4	49	14.1	< 3	40	34	30	52	14	4	< 0.1	< 0.5	6.1	0.91	1.56
3-27-08-4	Trx	320	0.007	0.7	2.8	< 3	5	38.4	7.5	< 3	40	30	25	44	7	3.6	< 0.1	1.4	5.5	0.74	1.59

All analyses by Activation Laboratories Ltd. (analysis code 4E: ICP, INAA, ICP/MS and XRF are all used for analysis)

*FUS: Sample preparation by lithium metaborate/tetraborate fusion. ICP: Analysis by inductively coupled plasma - mass spectrometry. INAA: Instrumental neutron activiation analysis.
TD: Total digestion by acid. MULT: Multicollector mass spectrometry.

TABLE 3. GEOCHEMISTRY SAMPLE LOCATIONS

Area	sample number	GPS station	NAD	Grid zone	UTM East	UTM North
Mammoth	3-26-08-2	JES-08-343	83	12	529187	3619953
Mammoth	3-26-08-3	JES-08-345	83	12	529042	3619652
Mammoth	3-26-08-5	JES-08-357	83	12	529506	3619876
Mammoth	3-26-08-6	JES-08-359	83	12	529613	3619931
Mammoth	3-27-08-1	JES-08-362	83	12	529748	3622599
Mammoth	3-27-08-2	JES-08-364	83	12	529697	3623279
Mammoth	3-27-08-3	JES-08-366	83	12	529707	3622151
Mammoth	3-27-08-4	JES-08-367	83	12	529765	3622180

GEOLOGIC MAP UNITS

Miscellaneous Quaternary Units

Plowed areas - Historically or actively plowed fields, irrigated pastures, and other lightly disturbed ground.

d **Disturbed ground (upper Holocene) -** Areas that have been modified by earth-moving equipment or otherwise modified due to mining activity or for road and housing construction.

collapsed ground - **Area of collapsed ground above underground ore-removal zone at San Manuel mine (upper Holocene) -** Area of collapsed ground above underground block-caving ore-removal zone at San Manuel mine

dc **Disturbed and collapsed ground, undivided (upper Holocene) -** Disturbed and collapsed ground associated with the San Manuel Mine.

mine dump - **Waste rock produced by mining (upper Holocene) -** Rock debris derived from ore-deposit overburden (mine waste).

mine tailings - **Tailings derived from processing ore from the San Manuel mine (upper Holocene) -** These tailings consist of ore rock that has been crushed to sand or silt size and from which most metal-sulfide minerals have been removed.

heap-leach pad - **Former heap-leach pad for oxide copper ore derived from the San Manuel ore body (upper Holocene) -** Former heap-leach pad for oxide copper ore derived from the upper part of the San Manuel ore body, now landscaped to resemble a hill.

Qtc - **Quaternary talus and colluvium (Holocene) -** Unconsolidated to weakly consolidated, very poorly sorted, angular, weakly bedded to massive, angular rock debris deposited at the base of bedrock slopes.

San Pedro River Alluvium

Qycr **Active river channel deposits -** Deposits are dominantly unconsolidated, very poorly sorted sandy to cobbly beds exhibiting bar and swale microtopography but can range from fine silty beds to coarse gravelly bars in meandering reaches based on position within the channel. Clasts are typically well-rounded but may be angular to sub angular. Qycr deposits are typically unvegetated to lightly vegetated and exhibit no soil development. Qycr deposits are entrenched from 30 cm to 5 meters or more below adjacent early historical floodplain deposits depending on location, geomorphic relationship, and local channel conditions. Although much of the San Pedro was a perennial stream historically, some sections are dry or marshy at the surface throughout much of the year. These deposits are the first to become submerged during moderate to extreme flow events and can be subject to deep, high velocity flow and lateral bank erosion.

Qy4r **Flood channel and low terrace deposits -** Deposits are found adjacent to active channels that form lightly vegetated in-channel bars, small planar fluvial terraces within 30 cm of river elevation, and recent erosional meanders outside the presently active channel. Terrace deposits are inset into older river alluvium and usually narrow, rarely more than 100 meters across. Qy4r deposits are composed of poorly sorted unconsolidated sediments ranging from fine silts to gravel bars depending on location in the channel at the time of deposition. Pebbles and cobbles are well-rounded to sub-rounded. These surfaces are commonly inundated under moderate to extreme flow events and can be subject to deep, high velocity flow and lateral bank erosion. These deposits do not exhibit soil development but may exhibit light vegetation cover consisting of small trees and bushes and grasses due to their relatively frequent inundation.

Qy3r **Historical river terrace deposits -** Terrace deposits occupying elevations from 1 to 2 meters above Qy4r deposits and inset below the pre-incision historical floodplain. These surfaces are generally planar but exhibit bar and swale microtopography. Although little to no soil development is present, dense grasses and small mesquite trees abound. Sediments composing these deposits are poorly sorted silt, sand, pebbles and cobbles. Pebbles and cobbles are well-rounded to sub-angular. Trough cross bedding, ripple marks, and stacked channel deposits viewable in cross-section indicate deposition in a low to moderate energy braided stream environment. These deposits are prone to flooding during extreme flow events, and undercutting and rapid erosion of Qy3r surfaces is possible during lower flow events.

Qy2r **Latest Holocene to historical river deposits -** Deposits associated with the floodplain that existed prior to the early historical entrenchment of the San Pedro River (Hereford, 1993; Huckleberry, 1996; Wood, 1997). Qy2r deposits are associated with broadly planar surfaces that locally retain the shape of historical river meanders. Qy2r surfaces are up to 7 meters above modern Qycr deposits and are the most extensive river terraces in the valley. Qy2r sediments were deposited when the San Pedro River was a widespread, shallowly-flowing river system and are dominated by fine grained floodplain deposits. Dense mesquite bosque and tall grass is typically present on these surfaces except where historic plowing or grazing has taken place. These surfaces appear predominantly fine grained at the surface due in part to the input of organic matter and windblown dust deposition but are composed of interfingering coarse sandy to pebbly braided channel and fine sand to silty river floodplain deposits. Where Qy2r deposits are moderately to deeply incised they not subject to inundation by river floods, but they may be flood-prone in areas with less channel incision. Qy2r deposits are subject to catastrophic bank failure due to undercutting and lateral erosion during flow events. Distal piedmont fan deposits (Qy2 ,Qyaf, and Qys) onlap onto Qy2r deposits although an interfingering relationship likely exits in the subsurface.

Qy1r **Late to early Holocene San Pedro terrace deposits -** Deposits associated with slightly higher terraces that represent either higher elements of the early historical floodplain or remnants of older Holocene aggradation periods. These fine-grained terrace deposits commonly have been disturbed by plowing or cattle grazing. When undisturbed, Qy1r deposits are densely vegetated by mature mesquite trees (mesquite bosque) and tall grasses. Soil development is moderate and surface color ranges from 10 to 7.5 YR 4/4. Due to the dense vegetation input of organic matter at the surface is high and often results in a thin (< 10 cm) organic soil horizon. A light dusting (incipient stage I) calcium carbonate accumulation is evident on the undersides of some buried clasts. Qy1r surfaces stand up to 7 meters above the active channel in highly incised locales and typically are located less than 1.5 m higher than adjacent Qy2r surfaces. These terraces are typically covered with fine-grained floodplain deposits, but relict gravel bars and lenses are common.

Qi3r **Late Pleistocene river terrace deposits -** Terrace deposits are up to 10 to 25 m higher than and up to 500 m outside the margins of the modern San Pedro channel. These deposits consist of well rounded pebbles to cobbles exhibiting stage I+ calcium carbonate accumulation with cross-bedded coarse sandy interbeds. Clast composition is varied and includes rock types not found in the mountains from which modern piedmont material is derived from. Qi3r terrace surfaces are planar, often surrounded by distal piedmont alluvium, and are generally lightly vegetated except for small weeds and grasses. Commonly, Qi3r deposits are inset into adjacent piedmont alluvial deposits but can also be inset into older river gravel terraces. Soil development is weak, possibly due to the porous nature of these deposits.

Qi2r **Middle to late Pleistocene river terrace deposits -** Terrace deposits are similar to Qi3r deposits but occupying higher positions in the landscape. Terrace surfaces are slightly to moderately rounded. Clast composition is diverse. Well-rounded pebbles to cobbles with stage I-II calcium carbonate accumulation armor Qi2r surfaces. Vegetation is sparse, consisting of small shrubs and grasses. Soil development is generally weak on Qi2r surfaces, but soil development is more evident in finer grained sections. Qi2r surfaces are typically found as high-standing isolated mounds surrounded by distal fan alluvium or as small terraces inset into older fan or basin fill alluvium.

Qi1r **Early to middle Pleistocene river gravel terraces -** Deposits are associated with high-standing, well-rounded river gravel terraces. Where Qi1r deposits are extensive, remnant planar caps are preserved near the center of the surface. Qi1r deposits are composed of very well rounded to well rounded pebbles and cobbles from diverse lithologies. Cross-bedded sands with pebbly stringers are interbedded throughout. Near-surface cobbly beds exhibit stage II+ calcium carbonate accumulation. Moderately to strongly calcium carbonate coated clasts or cemented aggregates of clasts mantle the flanks of Qi1r deposits, but clay accumulation is variable, probably due to poor surface preservation. Sparse small shrubs, weeds, and cacti are present on these surfaces.

Qi1r **Early to middle Pleistocene river deposits -** Fluvial facies includes moderately to well-cemented sandstone and conglomerate beds with river bedding structures, and lacks fine-grained deposits. River bedding structures include channel lag boulders in trough cross-beds overlain by climbing sets of tabular cross-beds (up to 1m thick). These deposits are scoured into Tqc and Tqp deposits and weather as a cliff-forming unit typically. In some localities a relict stage III+ to IV calcrete is present. Characteristic euhedral calcite crystals form interstitial cement commonly molded around clasts. The type locality for this facies is at the mouth of Tar Wash in the Mammoth Quadrangle. This facies can be laterally followed from the mouth of Tar Wash down the west flank of the San Pedro River. Paleo-flow directions are down-gradient to the northwest, sub-parallel to the San Pedro River. Paleo-gradients were not measured. This facies is interpreted to be lateral-bank fluvial deposits that mark the initial formation of the San Pedro River.

Piedmont Deposits

Qyc **Active tributary channel alluvium -** Unconsolidated, very poorly sorted sandy to cobbly piedmont channel sediments. Channels may exhibit bar and swale microtopography with bars composed of coarser sediments. Qyc deposits are typically unvegetated and exhibit no soil development although small shrubs and grasses can be found on slightly elevated bars. Qyc deposits commonly become submerged during moderate to extreme flow conditions and can be subject to deep, high velocity flow and lateral bank erosion. Channels are generally incised 1 to 2 m below adjacent Holocene alluvium and may be incised into adjacent Pleistocene alluvium by 10 m or more.

Qy3 **Latest Holocene alluvium -** Recently active piedmont alluvium located primarily along active tributary drainages including floodplain, low-lying terrace, and overflow channels. Qy3 deposits are composed of unconsolidated to very weakly consolidated silty to cobbly deposits and exhibit greater vegetation than Qyc deposits. These deposits generally exhibit bar and swale meso-scale topography and are susceptible to inundation during moderate to extreme flow conditions when channel flow exceeds capacity. Soil development is generally absent or incipient on Qy3 deposits which exhibit pale buff to light brown (10 YR) surface coloration.

Qy2 **Late Holocene alluvium** - Piedmont terrace deposits located primarily along the flanks of incised drainages and ephemeral floodplains, broad low-relief distal fan deposits onlapping onto Holocene river alluvium, and active tributary drainage deposits. These deposits consist of predominantly fine grained unconsolidated to weakly consolidated sediments although isolated sub-rounded to sub-angular cobbles and boulders may be present at the surface in small quantities. Where inset into older alluvium, Qy2 deposits are planar with remnant bar and swale meso-scale topography. Distal fan Qy2 deposits are broad and sandy with numerous small braided channel systems. Rarely active Qy2 tributary drainages are generally of limited extent, relatively steep, and more densely vegetated than Qy3 tributary drainages. Soil development on Qy2 deposits is weak, characterized by incipient stage I calcium carbonate accumulation in the form of small filaments and medium brown (10 YR) surface coloration. Vegetation on Qy2 surfaces ranges from numerous small mesquite trees and grasses in distal fan environments to medium creosote, acacia, and cholla in tributaries and inset terraces. These surfaces are subject to inundation during moderate to extreme flow conditions when channel flow exceeds capacity or due to channel migration on low-relief portions of broad distal fan deposits. Qy2 terraces are typically elevated from 30 cm to 1.5 m above active channels.

Qyaf **Late Holocene alluvial fan** - Qy2f deposits consist of active alluvial fan deposits in the San Pedro valley. These deposits have distributary drainage patterns and are prone to flooding and channel migration. Sediments are unconsolidated and consist of poorly sorted silt to cobbles. Vegetation includes small mesquite trees, shrubby acacia, prickly pear, and creosote.

Qy1 **Early to late Holocene alluvium** - Deposits consist of broad, low-relief, undulating fan deposits that sit higher in the landscape than younger Holocene alluvium. Portions of these deposits are mantled by coarse to very coarse angular quartz sand and exhibit diverse vegetation patterns dominated by cholla, prickly pear, small (1-1.5 m tall) mesquite, and numerous small shrubs and grasses. Overall relief between broad fan crests and incised drainages on gently rolling Qy1 deposits typically does not exceed 1.5 meters. Numerous shallow braided channels drain widespread portions of Qy1 surfaces. Qy1 deposits exhibit incipient calcium carbonate accumulation (stage I) and soil development characterized by medium brown (10-7.5 YR) coloration where unincised. Deposition of Qy1 sediments in a braided channel aggrading alluvial fan environment has, in places, resulted in shallow burial of adjacent piedmont deposits. This relationship is visible along incised channels where thin Qy1 deposits overly redder, grusy, clay-rich Qi2 or Qi3 deposits.

Qi3 **Late Pleistocene alluvium** - Qi3 deposits form widespread planar reddish fan terraces mantled by angular to sub-angular pebbles to boulders. These deposits exhibit moderate calcium carbonate accumulation (stage I to II) and soil development with reddish shallow subsurface coloration (7.5 YR 4/4). This color varies with position in the piedmont due to differences in parent material (mixed granitic, metamorphic and volcanic clasts west of San Pedro and volcanic clasts to the east). Qi3 deposits have saguaro, palo verde, mesquite, cholla, prickly pear, creosote, acacia, and numerous small grasses and shrubs. Qi3 deposits stand up to 5 to 20 meters higher in the landscape than adjacent Qy1 and Qyc deposits depending on local incision and position within the piedmont.

Qi2 **Middle to late Pleistocene alluvium** - Qi2 deposits form broad planar fan and terrace surfaces that cap Quiburis basin fill deposits. These deposits generally exhibit reddish (5 YR 5/4) soils and moderate calcium carbonate accumulation (stage I to IV). Varnish and pavement development is moderate to poorly exhibited. Qi2 deposits are overall planar but can exhibit mild to moderate rounding near incised channels or inset terraces. Vegetation on Qi2 surfaces consists of saguaro, palo verde, medium mesquite, prickly pear, cholla, barrel cactus, and numerous small shrubs and short grasses. Where incised, these deposits often exhibit a cap up to 2 meters thick of moderately calcium carbonate cemented clasts. This cap preserves underlying, less-indurated portions of the Qi2 surface as well as any deposits it may overly. Qi2 terraces deposited onto basin fill deposits may stand as much as 30 to 50 meters above active piedmont channels.

QTa **Quaternary-Tertiary alluvium -** Old alluvial deposits and veneer which overlie bedrock and Quiburis basin-fill conglomeratic facies and form the upper parts of high, very rounded ridges. QTa deposits are composed of a reddish tan, non-indurated, carbonate-cemented fanglomerate cap consisting of coarse sand and gravel. In some areas the unit appears as a lag of resistant clasts weathered from the Quiburis conglomeratic facies. Exposures of QTa deposits are generally poor, but they may locally be at least 10 to 30 meters thick and are commonly the highest standing deposits in the proximal piedmont.

Basin-Fill Deposits

Tqc **Late Miocene to Pliocene Quiburis deposits, conglomeratic facies -** Sandy conglomerate, conglomeratic sandstone, some sandstone, rare mudrock formed as alluvial fans and braidplain deposits. Generally very light gray and moderately to strongly indurated. Outcrops of Tqc weather moderately to well rounded. Sand is poorly sorted, angular, medium grained to granule sand, with abundant disaggregated granite particles of quartz or feldspar. Clasts in conglomerate typically include significant percentage of Oracle granite, also Cloudburst volcanics, and sparse Apache Group clasts. Percentages of granite and volcanics vary as much as 50% depending on location and proximity to source terrain. Bedding generally massive yet distinguishable by grain size variations, locally by parting between beds. Tqc overlies the fan toe and sandflat facies gradationally where interbedding of the two facies is common near the contact, most noticeably near cliffs, between the mouths of Tar and Tucson washes.

Tqs **Late Miocene to Pliocene Quiburis deposits, sandflat facies -** Distal-fan and deltaic sandflat and lake margin facies include massive to laminated sandstone, siltstone, mudstone, and gypsum. This facies varies in grain size, relative distribution and depositional environment between laterally equivalent alluvial-fan/braidplain (Tqc) and lacustrine (Tql) facies. Interstitial gypsum in fine-grained clastic deposits is common and characteristic of these distal fan- to basin-axis deposits. Volcanic ash beds have been documented in this facies and are locally reworked into clastic beds. Tqs weathers commonly into slopes, although where gypsum, massive siltstone and sandstone predominate, cliff and stair-step exposures appear to be more common. Tqs is in gradational contact between the overlying conglomeratic and underlying lucustrine facies where lithologies associated with each facies are commonly interbedded.

Tql **Late Miocene to Pliocene Quiburis deposits, lacustrine facies -** Laminated lacustrine facies includes interbedded mudstone, limestone, gypsum, and diatomite beds of varying thickness, with sparse and thin intercalations of laminated lacustrine sandstone. Diatomite beds range from 20 cm to 1 m thick. Where diatomite beds interbedded with siltstone dominate this facies exhibits a characteristic white outcrop color, although silt and mud commonly coat outcrop surfaces. Diatomite beds are resistant to weathering and commonly form cliff-slope-cliff topography. Relatively softer beds are composed of a mix of mudstone, siltstone, and limestone. Rare beds of soft, unconsolidated volcanic ash are preserved best underlying resistant beds of gypsiferous siltstone and diatomite. Insects commonly burrow in the volcanic ash layers.

Miocene San Manuel Formation

Tst **San Manuel Formation, Tucson Wash Member -** Conglomerate and conglomeratic sandstone derived from Cloudburst and Galiuro Volcanics. Paleocurrent directions, indicated by clast imbrication, are dominant southwesterly (Dickinson, 1993).

Tsk **San Manuel Formation, Kannally Member -** Conglomerate and conglomeratic sandstone derived largely from Oracle Granite. Paleocurrent directions, indicated by clast imbrication, are dominantly east-northeast (Dickinson, 1993).

Tsc **Weakly to moderately indurated, volcanic-lithic conglomerate -** Mostly volcanic lithic (andesitic) conglomerate, locally contains abundant Tertiary intrusive rhyolite clasts. Unit is exposed in a small area around the Tiger Mine north of the San Manuel mine. Bedding is defined by grain-size variations and clast alignment. Generally medium gray color, weathered surfaces look like colluvium on Cloudburst volcanic rocks. This unit is less indurated and altered than Cloudburst conglomerate, and lacks abundant granitic detritus typical of Quiburis Formation.

Oligocene to lower Miocene igneous and sedimentary units

Tri **Intrusive rhyolite -** White to light gray, very fine grained rhyolite, with 1-2% phenocrysts of quartz, feldspar, and trace biotite, in variable ratios. Quartz is usually the most easily discerned phenocryst. Locally this unit includes zones of intrusive breccia, and grades into intrusive breccia of map unit Trix. Chemical analysis (Fig. 2; Table 1) indicates that this unit is well within the rhyolite field of Le Bas et al. (1986). This unit includes scattered rhyodacitic intrusions mapped by Creasey (1965).

Trix **Intrusive rhyolitic breccia -** Rhyolite, monolithologic breccia derived from rhyolite, and heterolithologic breccia derived from rhyolite, mafic volcanic rocks (Cloudburst volcanics), and Oracle Granite. Matrix is very fine grained rock of generally undiscernible igneous or fragmental origin, with sparse quartz phenocrysts. Locally the unit consists of clearly intrusive rhyolite. Contacts are sharp or gradational into unbrecciated country rock or Cloudburst volcanic or sedimentary rock. Field relationships indicate that this unit was emplaced in the subsurface as dikes and plugs. Structure to some breccia that resembles bedding is interpreted to represent processes associated with entrainment of wallrocks and incomplete rock-fragment mixing during possibly violent brecciation and ascent within gas-charged magma.

Trx **Intrusive rhyolite and rhyolite breccia, undivided -** Intrusive rhyolite and rhyolite breccia, undivided. Locally this unit includes breccia that is layered and appears to be bedded. However, association with far more voluminous massive breccia, and highly indurated nature of all breccia, suggests that layering is the result of processes that occurred in the subsurface during magma and breccia ascent, possibly in a gas-charged magma conduit with voids in which breccia-fragment layering developed in small areas. Chemical analysis (Fig. 2; Table 1) indicates that this unit is well within the rhyolite field of Le Bas et al. (1986).

Tcs **Cloudburst Formation, sedimentary unit -** Conglomerate and sandstone representing alluvial fan and braidplain facies (Dickinson, 1993) and derived primarily from mafic Cloudburst volcanics. This unit locally includes abundant debris derived from Oracle Granite, and probable debris flows and rock avalanche breccias. Paleocurrent directions are toward the north-northeast except in the upper Tucson Wash area (south of Black Canyon fault) where they are toward the northwest (Dickinson, 1993).

Tcsg **Cloudburst Formation, granitic sediment facies -** Conglomerate and breccia derived from Oracle Granite and interbedded with Cloudburst volcanics. A several-hundred-meter-long sheet of this rock unit south of Tar Wash and within Cloudburst volcanics consists of two slabs of solid to shattered Oracle Granite, each 20m to 30m x 100m to 200 m in size, and associated conglomerate (this granite and granite breccia had been mapped as fault-bounded bedrock by Creasey (1965)).

In the Tiger Mine area, this unit includes basaltic lava, some fragmental rock, with lenses or layers of red brown to dark brown granule pebbly sandstone to sandy conglomerate. Abundant 1-5 mm quartz and feldspar derived from erosion of granite, as well as pebbles to boulders of Oracle granite, are ubiquitous in clastic rocks, along with rare to abundant basaltic clasts. This is the facies observed to overlie granite in the Tiger Pit.

Tcv **Cloudburst Formation, volcanic unit -** Massive, crystal-poor to slightly porphyritic, medium to dark gray lava flows and autobreccia, and less abundant volcanic-lithic breccia and massive conglomerate. Phenocrysts include 2-3%, 1 mm-diameter, brown, altered, orthopyroxene? or olivine?, 5-7%, green, 1-3 mm-diameter, altered clinopyroxene(?), 1-2 mm-diameter orthopyroxene(?) altered to greasy grey and brown alteration products, and minor 2-mm-diameter plagioclase.

Tcvc **Cloudburst Formation, massive volcanic conglomerate -** Massive to crudely bedded, polymict boulder conglomerate with mafic volcanic clasts and minor Oracle granite grus and clasts.

Tcvs **Cloudburst formation, volcanic, volcaniclastic, and brecciated rocks, undivided -** Undivided mafic lava flows, rhyolite intrusions, and massive breccia derived from highly variable proportions of rhyolite, Cloudburst volcanics, and Oracle Granite ("three-bean breccia"). In places this unit is cut by rhyolite dikes, in other places the breccia incorporated rhyolite fragments. This relationship is interpreted to indicate that the breccia was produced by processes associated with rhyolite (unit Tri) emplacement and rhyolite brecciation (unit Trx) and incorporation of wall rocks into rhyolite breccia and partial mixing with the breccia during transport and emplacement (unit Trix).

A large block of Oracle Granite within the breccia is mapped separately. This block is cut by a deep slot on the east side of Tucson Wash about 200 m north of where Tucson Wash crosses the Turtle fault. In this slot an exposure of a fault places Oracle Granite against Oracle Granite and is interpreted as a segment of a fault that was broken from its original location and carried upward within the ascending breccia. Weak chloritic alteration suggests that this fault segment was originally associated with the Cloudburst detachment fault.

Tcmf **Cloudburst formation, mafic fragmental rock -** Massive monolithologic fragmental rock derived from mafic Cloudburst volcanics, locally with sparse clasts of other rock types. At least some of this unit is interpreted as autobreccia, but association with heterolithologic breccia of map unit Tcvs and local inclusion of minor amounts of other rock types suggests that some of this unit is a monolithologic equivalent of the heterolithologic breccia unit.

md **mafic dike -** Mafic dike containing fine- to medium-grained plagioclase phenocrysts, possibly with hornblende and/or biotite. Some of these dikes were mapped as diabase by Creasey (1965) but are also shown as cutting across Laramide granodiorite porphyry, which indicates that the dikes are not related to the common, Mesoproterozoic Sierra Ancha diabase of southeastern Arizona. Age is uncertain but dikes are suspected to be related to the Cloudburst volcanics.

cc **Undesignated crystalline carbonate -** Bedded and brecciated crystalline limestone with interstitial chert along bedding planes. Bedding is thin, medium and massive. Texture of limestone and possibly dolomite is spar-rich, no micrite. Fine-grained chert weathers to a distinctive orange color. Bedding where preserved is laminar to planar with minor cross-lamination within 10-cm beds. One 15-cm bed of intraclastic limestone observed overlain unevenly by a 3 to 5-cm horizon of glauconite, indicating a shallow-marine depositional environment. The outcrop is upright and a coarse limestone-breccia (lacking chert) forms the upper portion of the outcrop where it is faulted against weathered Oracle Granite. The base of the limestone is in contact with similar granite; the relationship of the contact is unknown, however, differential weathering at the base of the limestone with the granite suggests the contact may be nonconformable. The limestone outcrop is moderate to highly fractured. Possible ages include Proterozoic, Paleozoic or Oligo-Miocene. A younger age is precluded by hydrothermal alteration and recrystallization, which has not affected any of the abundant Pliocene Quiburis Formation.

Laramide units (upper Cretaceous and lower Tertiary)

Kaf **American Flag Formation** - Conglomerate with clasts of Oracle Granite and volcanic rocks overlain by intermediate volcanics and lava autobreccia (Force, 1997). Located southeast of the San Manuel mine, these strata were mapped as Cloudburst Formation by Creasey (1965) but were determined to be intruded by the 68 Ma San Manuel Porphyry and correlated with the Laramide American Flag Formation (Force, 1997; Unruh, 1997).

TKgp **Granodiorite porphyry** - Granodiorite porphyry with abundant plagioclase up to 7 mm, less common biotite and hornblende, in a fine-grained gray groundmass that contains fine quartz and K-feldspar as well as plagioclase and mafic minerals (Creasey, 1965). According to Creasey (1965) most exposures of the map unit contain both biotite and hornblende, but some contain only biotite. This unit forms most of the pit at the San Manuel mine, but was mapped there by S. Skotnicki (for SRK) as "dacite porphyry". Two samples of the granodiorite porphyry, from locations in the footwall and hanging wall of the San Manuel fault, yielded U-Pb zircon dates of 68.1 ± 3.0 Ma and 67.8 ± 2.3 Ma (Force, 1997; Unruh, 1997).

Proterozoic units

Aplite dikes - Light cream or buff colored, fine to medium grained, aplite dikes with a saccharoidal (aplitic) texture (Creasey, 1965). One sample was described by Creasey (1965) as consisting of 59% albite (An_3), 40% quartz, 1% opaque minerals, and <1% K-feldspar.

Yd **diabase** - Dark greenish gray to olive gray to black, fine to medium grained diabase dikes within Oracle Granite. Creasey (1965) determined that three samples consist of 35-55% plagioclase, 61-25% hornblende, and 4-8% opaque minerals, with mafic constituents interstitial to acicular plagioclases (An_{35-40} for one sample).

Yo **Oracle Granite** - Porphyritic, medium- to coarse-grained biotite granite ("quartz monzonite" of Creasey [1965]).

Similar granite in the Samaniego Hills, 100 km to the west, has been dated by U-Pb zircon at 1434.5 ± 3.4 Ma. Two-mica granite at Black Mountain, located 20 km to the west and interpreted as a phase of Oracle Granite, has been dated by U-Pb zircon at 1433.5 ± 2.1 Ma (Spencer et al., 2003). This is the inferred to be the age of the Oracle Granite.

Yoa **Oracle Granite, alaskitic** - Equigranular, medium to coarse grained, pale gray alaskite that forms an irregular intrusion in the northwestern part of the map area. This unit was described by Creasey (1965) as saccharoidal near its margins and porphyritic in its interior exposures, and as consisting of 24% plagioclase, 43% quartz, 31% K-feldspar, 1% hornblende, and 1% chlorite.

Yogd **Oracle Granite, granodioritic** - Medium-grained, gray granodiorite containing biotite and hornblende. Creasey (1965) described this rock unit as hypidiomorphic granular, with $An_{30} \pm 5$, ~18% biotite, and ~13% mafic (biotite + hornblende).

References Cited

Creasey, S. C., 1965, Geology of the San Manuel area, Pinal County, Arizona: U. S. Geological Survey Professional Paper 471, 64 p., with map, scale 1:24,000.

Dickinson, W.R., 1993, Summary geologic map of Black Hills near Mammoth, Pinal County, Arizona [Mammoth 7.5 min]: Arizona Geological Survey Contributed Map CM-93-B, 1 sheet, scale 1:24,000.

Force, E.R., 1997, Geology and mineral resources of the Santa Catalina Mountains, southeastern Arizona: Tucson, Arizona, Center for Mineral Resources, Monographs in Mineral Resource Science, n. 1, 134 p.

Hereford, R., 1993, Entrenchment and widening of the upper San Pedro River, Arizona: Geological Society of America Special Paper 182, 46 p.

Huckleberry, G., 1996, Historical channel changes on the San Pedro River, southeastern Arizona (revised October 1996): Arizona Geological Survey Open-File Report 96-15, 22 p.

Le Bas, M.J., Le Maitre, R.W., Streckeisen, A., and Zanettin, B., 1986, A chemical classification of volcanic rocks based on the total alkali-silica diagram: Journal of Petrology, v. 27, p. 745-750.

Spencer, J.E., Isachsen, C.E., Ferguson, C.A., Richard, S.M., Skotnicki, S.J., Wooden, J., and Riggs, N.R., 2003, U-Pb isotope geochronologic data from 23 igneous rock units in central and southeastern Arizona: Arizona Geological Survey Open-File Report 03-08, 40 p.

Unruh, D.M., 1997, Porphyry geochronology and geochemistry, *in* Force, E.R., Geology and mineral resources of the Santa Catalina Mountains, southeastern Arizona: Tucson, Arizona, Center for Mineral Resources, Monographs in Mineral Resource Science, n. 1, p. 94-100.

Wood, M.L., 1997, Historical channel changes along the lower San Pedro River, southeastern Arizona: Arizona Geological Survey Open-File Report 97-21, 44 p., 3 sheets, scale 1:24,000.